PROGRAMME

Konferens i Mineralteknik
Conference in Minerals Engineering

7–8 February 2023

Mineralteknik/Mineral Processing

ltu.se/minpro

LULEÅ TEKNISKA UNIVERSITET

Wednesday, February 8, 2023

Session 3 – Industrial projects

Session chair: Laurindo de Salles Leal Filho

08.45 – 09-15	Mohammad KHOSHKHOO, BOLIDEN MINERAL AB *Bioleaching: A Promising Option for Recovery of Valuables from Sulphidic Residues*
09.15 – 09.45	Ulrika HÅKANSSON, LKAB MINERALS *Circular Production of Phosphorus and Rare Earth Elements*
09.45 – 10.15	Mohammad JOOSHAKI, GTK *Digitization and Automation of GTK's Mineral Processing Pilot Plant and Research Laboratories – for Improving Productivity and Customer Experience*
10.15 – 10.45	Coffee break

Session 4 – Particles and simulation

Session chair: Jan Rosenkranz

10.45 – 11.15	Per SVEDENSTEN, NMS RESEARCH CENTER *New Crusher Simulation Model for Improved Flowsheet Simulation Accuracy*
11.15 – 11.45	Magnus EVERTSSON, CHALMERS *Characterization of Single Particle Breakage for Improved Energy Efficiency in Comminution*
11.45 – 12.15	Raimon TOLOSANA-DELGADO, HZDR *Particle-based process understanding and geometallurgical testing*
12.15 – 13.15	Lunch at Bistron

Session 5 – Battery technology

Session chair: Saeed Chelgani

13.15 – 13.45	Mohamed ELSADEK, LTU *Recovery of Valuable Metals from Spent LIBs Black Mass Using Thermal Treatment*
13.45 – 14.15	Allan GOMEZ-FLORES, HANYANG UNIVERSITY *Simulating the Separation of Black Mass Particles Using CFD*
14:15 – 14:45	Gilsang HONG, HANYANG UNIVERSITY *Direct Separation of Cathode and Anode Active Materials of Spent Lithium Ion Batteries*
14.45 – 14.50	Conference closing

15:00 (15:20) LLT-buss till Luleå Airport (Linje 4)/LLT-bus to Luleå Airport (Nr 4)
Avgår var 20:e minut / Departure every 20th minute

Simulating the separation of black mass particles using CFD

Allan Gomez-Flores[a], Gilsang Hong[a], Hyun-Su Park[a], Hee-Eun Jung[a], Junseop Lee[b], and Hyunjung Kim[a,*]

[a] Department of Earth Resources and Environmental Engineering, Hanyang University, 222 Wangsimni-ro, Seongdong-gu, Seoul 04763, Republic of Korea

[b] Technology Planning Team, Korea Mine Rehabilitation and Mineral Resources Corp., Wonju, Gangwon-do 26464, Republic of Korea

* Corresponding author. Tel.: +82-2-2220-0541, Fax: +82-2-2220-3119, E-mail: kshjkim@hanyang.ac.kr

ABSTRACT

Discarded lithium-ion batteries can be recycled to recover minerals such as graphite, Li, Ni, Mn, and Co, improving mineral supply and promoting a cleaner environment. Black mass consisting of NMC (Li-Ni-Mn-Co oxide) and graphite particles mixed with an organic polymer binder, can be obtained from these batteries through a process of comminution and thermal treatment. Flotation can be used to separate minerals in black mass. By simulating the flotation process using computational fluid dynamics and a flotation kinetic model, we were able to predict the separation of graphite particles from NMC. However, some NMC was also recovered due to its surface properties and entertainment. Future studies will focus on reducing NMC recovery by analyzing hydrodynamic and pulp chemistry conditions.

1 Introduction

End-of-life NMC batteries can be recycled through a process involving pretreatment and flotation. Pretreatment includes comminution, collection of the <100 μm fraction, and Fenton, grinding, or heat (~500 °C) treatments. The product of pretreatment is called black mass, which contains anode (graphite) and cathode (NMC) particles. The organic binder provides hydrophobicity to both graphite and NMC particles, hindering their selective separation by flotation. Therefore, black mass is treated with heat to remove the organic binder, improving particle liberation, which is beneficial for flotation. For pure mineral particles, NMC particles are hydrophilic and graphite particles are hydrophobic. However, NMC recovery can occur due to the remaining binder on their surface. There are works that investigated the flotation of black mass from NMC batteries [1, 2] and others (e.g., $LiFeO_4$ or $LiCoO_2$ batteries) [3-5]. These works revealed that cathode (Li oxides) particles can also be recovered by entrainment, decreasing the grade of the graphite concentrate. Therefore, we aimed to investigate hydrodynamic and physicochemical conditions that contribute to NMC recovery.

2 Materials and methods

Simulations of flotation in a Denver type cell at laboratory scale were carried out using COMSOL 6.1. A two-phase mixture k-epsilon turbulence model was used to simulate water-bubbles and water-solids mixtures; the results of these simulations were combined in a kinetic study using a flotation model [6-8]. The water-solids mixture simulation considered three

particle types concurrently. The flotation model considered pulp and surface chemistry through the extended Derjaguin−Landau−Verwey−Overbeek (XDLVO) theory. Table 1 summarizes the conditions and particles properties used for the simulations.

Table 1. Simulation conditions and particle properties used for simulations.

Variable	Value
Air flux	2×10^{-4} kg/s
Bubble diameter (assumed constant due to frother)	5×10^{-4} m
Particle 1 (graphite) diameter	1×10^{-5} m
Particle 2 (graphite) diameter	4×10^{-5} m
Particle 3 (NMC) diameter	1.244×10^{-5} m
Particle 1 density	2350 kg/m^3
Particle 2 density	2210 kg/m^3
Particle 3 density	4698 kg/m^3
Particle 1 volume fraction	0.6120
Particle 2 volume fraction	0.0306
Particle 3 volume fraction	0.06120
Impeller rotating speed	1200 rpm
Bubble zeta potential	-32 mV
Particle 1 zeta potential	-20 mV
Particle 2 zeta potential	-35 mV
Particle 3 zeta potential	3 mV
Pulp ionic strength (assuming NaCl)	0.1 mmol/l
Particle 1 combined Hamaker constant	-6.0116×10^{-21} J
Particle 2 combined Hamaker constant	-6.0116×10^{-21} J
Particle 3 combined Hamaker constant	-1.4708×10^{-21} J
Particle 1 contact angle	80 degrees
Particle 2 contact angle	80 degrees
Particle 3 contact angle	10 degrees
Particle 1 combined hydrophobic constant	6.0878×10^{-20} J
Particle 2 combined hydrophobic constant	6.0878×10^{-20} J
Particle 3 combined hydrophobic constant	1.2775×10^{-25} J

3 Results and discussion

Figure 1 shows a cross sectional view of the velocity and turbulence of the water-bubble mixture inside the Denver flotation cell. Higher velocities and turbulence were present near the impeller, suggesting that bubble-particle interactions will mostly occur in this area.

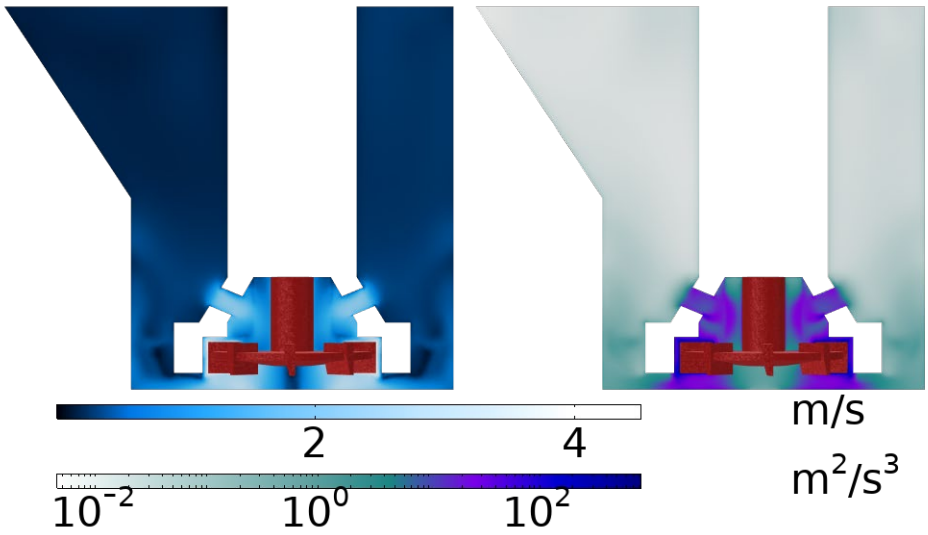

Figure 1. Water-bubble mixture velocity magnitude (m/s) and turbulence (m^2/s^3 in logarithmic scale) inside the Denver flotation cell.

Figure 2 shows the XDLVO profiles of bubble-particle interactions. Particle 1 had a strong attraction to a bubble because there was no energy barrier, while particles 2 and 3 had energy barriers that must be overcome to attach to a bubble. An energy barrier can be overcome if sufficient kinetic energy is provided. Particle 3 exhibited a strong repulsion at separation distances <0.1 nm due to the repulsive Hamaker constant between the bubble and particle, while particles 1 and 2 did not exhibit this strong repulsion because the stronger hydrophobic interaction overcomes the repulsive Hamaker constant (see Table 1).

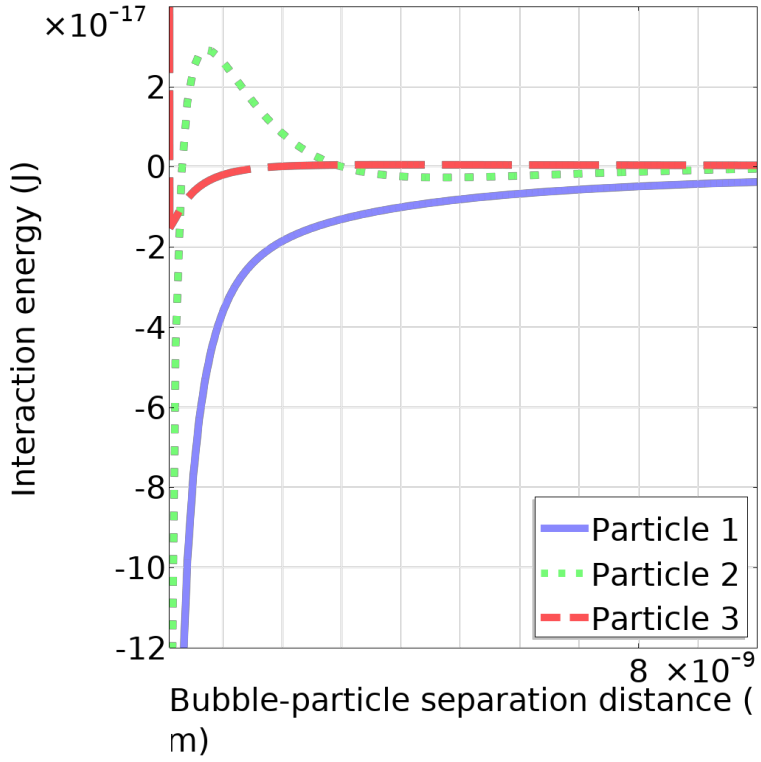

Figure 2. XDLVO (van der Waals, electrostatic, hydrophobic) profiles of bubble-particle interactions.

Figure 3 shows collision probabilities (P_c) of bubble-particle interactions inside the Denver flotation cell. Particles 1 and 3 had low P_c due to their small diameter (~10 microns), while particle 2 had a higher P_c due to its larger diameter (40 microns).

Also, Figure 3 shows attachment probabilities (P_a) of bubble-particle interactions inside the Denver flotation cell. Particle 1 had the highest P_a because it had no energy barrier hindering its attachment to a bubble, while particles 2 and 3 had energy barriers that hindered their attachment to bubbles. Particle 2 had a much higher energy barrier than particle 3. These energy barriers are overcome near the impeller blades due to the high velocities and turbulence. Increasing salt concentration can increase particle 2 attachment by decreasing the energy barrier due to reduced electrostatic repulsion and improving binder removal can decrease particle 3 attachment by increasing the energy barrier due to increased hydrophilicity.

Figure 3 also shows stabilization probabilities (P_s) of bubble-particle interactions inside the Denver flotation cell. Particles 1 and 2 were very stable once attached due to their high contact angle (see Table 1), but some detachment can occur near the blades and impeller due to the high velocities and turbulence. Particle 3 had low P_s due to its low contact angle (see Table 1).

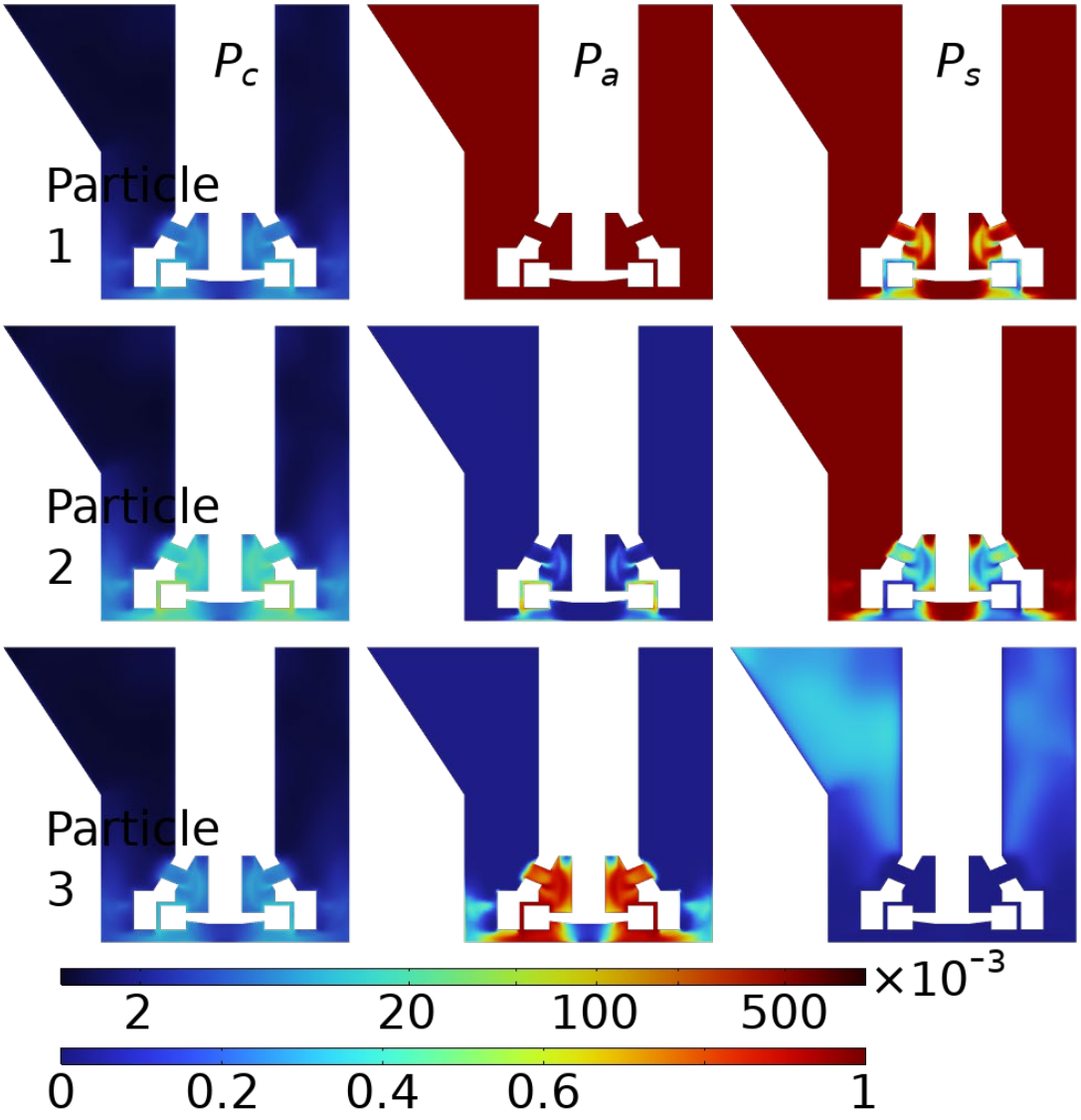

Figure 3. Probabilities of collision (P_c in logarithmic scale), attachment (P_a), and stabilization (P_s) of particles inside the Denver flotation cell.

Figure 4 shows the fraction of floated particles inside the Denver flotation cell during 320 seconds of simulation. Particle 1 was almost completely recovered, while particle 2 was partially recovered due to its low P_a. Particle 3, which is undesirable in the concentrate, had some recovery (~5%) due to its P_a. Figure 5 shows the flotation recovery considering particle entrainment [8] inside the Denver flotation cell during 320 seconds of simulation. The pulp and entrainment recoveries of particle 1 (10 microns) were higher than those of particles 2 (40 microns) and 3 (~12 microns) due to their small size. While particle 3 was susceptible to entrainment, its higher density (see Table 1) significantly reduces its entrainment recovery. Therefore, any recovery of NMC particles in the graphite concentrate is attributed to pulp and particle surface chemistry, which can be carefully modified with physicochemical knowledge to improve the grade of the graphite concentrate.

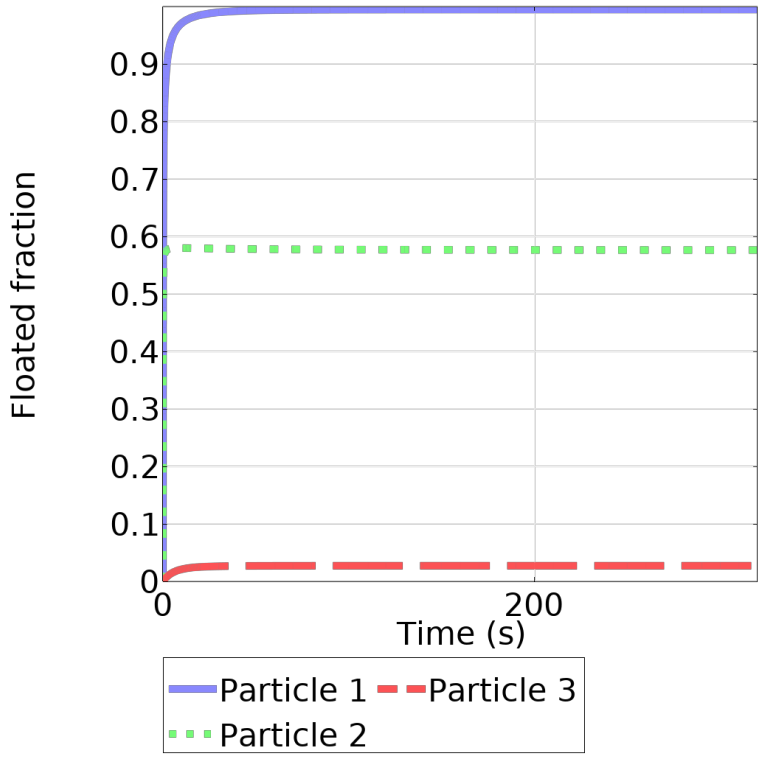

Figure 4. Floated fraction of particles inside the Denver flotation cell during 320 seconds of simulation.

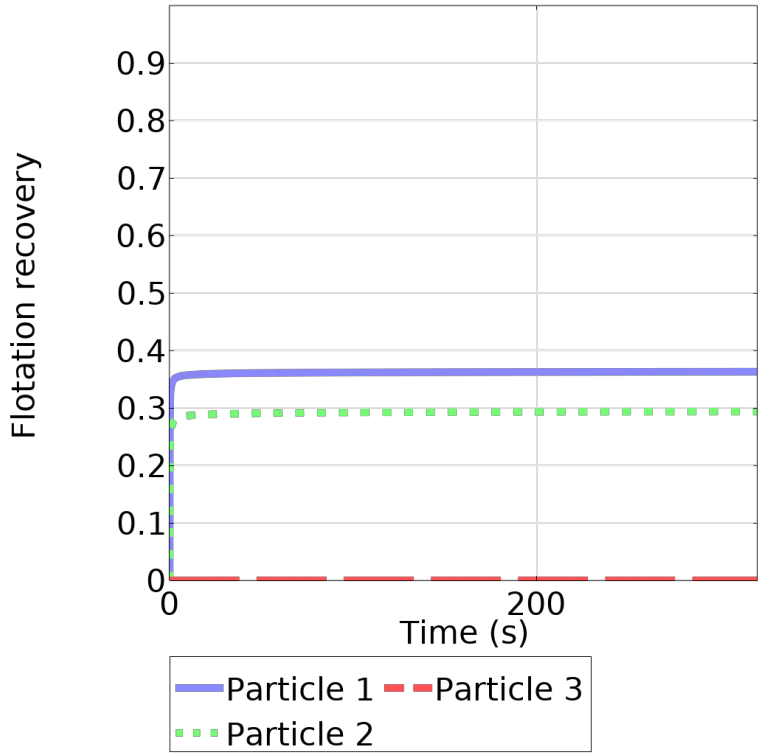

Figure 5. Flotation recovery of particles considering entrainment inside the Denver flotation cell during 320 seconds of simulation.

Table 2 presents the flotation probability (P_k) of particles inside the Denver flotation cell. Froth recovery (R_f) from simulations included recovery due to bubble-particle attachment in froth phase and recovery due to entrainment. It was found that P_k followed the order particle 3 < particle 2 < particle 1. P_k cannot be related to P_c, P_a, and P_s because they were defined differently. Specifically, P_k was obtained from the total particle number decrease rate due to multiple encounters over time, while P_c, P_a, and P_s were the result of a single encounter [7]. Reference 7 presented P_k as a formula assuming R_f=1, resulting in P_k values of 0.10353, 0.082821, and 5.5214×10^{-6} for particles 1, 2, and 3, respectively (see Table 2). In future studies, the definition of P_k in the kinetic model used in our study should be thoroughly investigated and potentially revised.

Table 2. Estimated flotation bubble surface area flux, rate coefficients, averaged (320 s) froth recoveries, and flotation probabilities of particles inside the Denver flotation cell.

Variable	Particle 1	Particle 2	Particle 3
Bubble surface area flux, S_b (1/s)		83.692	
Flotation rate coefficient, k (1/s)	8.6643	6.9315	0.004621
Froth recovery, R_f (-)	0.93440	0.71887	1.835×10^{-6}
Flotation probability, $P_k=k/(S_b\cdot R_f)$ (-)	0.11079	0.11521	30.089
P_k assuming R_f=1 as in reference 7	0.10353	0.082821	5.5214×10^{-6}

4 Conclusions

Particle 1, followed by particle 2, was more susceptible to entertainment due to their size and density, while particle 3 was not due to its higher density. Ideally, there should be no recovery of particle 3 in a graphite concentrate to achieve full separation of anode and cathode particles. Nevertheless, some recovery occurs due to its surface properties that allow it to attach to bubbles and float. Therefore, modifications to pulp chemistry and surface chemistry can affect bubble-particle interactions, influencing particle recovery and concentrate grade. Further research on (i) physicochemical conditions that improve flotation separation, as well as (ii) binder removal methods and (ii) how it remains on cathode particles in black mass, should be conducted.

Acknowledgements
This work was supported by the R&D Project of the Korea Mine Rehabilitation and Mineral Resources Corporation in 2022 and the framework of international cooperation program managed by the National Research Foundation of Korea (NRF-2022K2A9A2A12000254).

References

[1] Verdugo, L., Zhang, L., Saito, K., Bruckard, W., Menacho, J., & Hoadley, A. (2022). Flotation behavior of the most common electrode materials in lithium ion batteries. Separation and Purification Technology, 301, 121885.
[2] Qiu, H., Peschel, C., Winter, M., Nowak, S., Köthe, J., & Goldmann, D. (2022). Recovery of Graphite and Cathode Active Materials from Spent Lithium-Ion Batteries by Applying Two Pretreatment Methods and Flotation Combined with a Rapid Analysis Technique. Metals, 12(4), 677.
[3] Zhong, X., Mao, X., Qin, W., Zeng, H., Zhao, G., & Han, J. (2023). Facile separation and regeneration of LiFePO4 from spent lithium-ion batteries via effective pyrolysis and flotation: An economical and eco-friendly approach. Waste Management, 156, 236-246.
[4] Vanderbruggen, A., Hayagan, N., Bachmann, K., Ferreira, A., Werner, D., Horn, D., ... & Rudolph, M. (2022). Lithium-Ion Battery Recycling─ Influence of Recycling Processes on Component Liberation and Flotation Separation Efficiency. ACS ES&T Engineering, 2(11), 2130-2141.
[5] Zhang, G., Ding, L., Yuan, X., He, Y., Wang, H., & He, J. (2021). Recycling of electrode materials from spent lithium-ion battery by pyrolysis-assisted flotation. Journal of Environmental Chemical Engineering, 9(6), 106777.
[6] Gomez-Flores, A., Solongo, S. K., Heyes, G. W., Ilyas, S., & Kim, H. (2020). Bubble–particle interactions with hydrodynamics, XDLVO theory, and surface roughness for flotation in an agitated tank using CFD simulations. Minerals Engineering, 152, 106368.
[7] Koh, P. T. L., & Schwarz, M. P. (2006). CFD modelling of bubble–particle attachments in flotation cells. Minerals Engineering, 19(6-8), 619-626.
[8] Yoon, R. H., Soni, G., Huang, K., Park, S., & Pan, L. (2016). Development of a turbulent flotation model from first principles and its validation. International Journal of Mineral Processing, 156, 43-51.